

# Pattern association by a lateral-alignment-free optical neural network

N. Tsumura, Y. Fujii, K. Itoh, Y. Ichioka

Department of Applied Physics, Osaka University, Japan

**Pattern association by a lateral-alignment-free optical neural network.** We propose an optical technique that solves partially the problem of alignment of optical neural networks. The synaptic weights are recorded on a special SLM that is located between input and output layers of optical artificial neurons. The SLM can accept the optical signals for changing the synaptic weights from both the input and output layers. The positions of synaptic weights to be recorded are automatically aligned by the positions of the neurons in the both layers. Results of an association experiment from Chinese characters to alphabets are presented.

**Musterverknüpfung durch ein seitwärts ausrichtungsfreies optisches neuronales Netz.** Wir schlagen eine optische Technik vor, die teilweise das Problem der Ausrichtung optischer neuronaler Netze löst. Die synaptischen Gewichte werden auf einem speziellen SLM aufgenommen, der sich zwischen Eingangs- und Ausgangsschichten der optischen künstlichen Neuronen befindet. Der SLM kann die optischen Signale zum Wechsel der synaptischen Gewichte von den Eingangs- wie von den Ausgangsschichten registrieren. Die Position der zu registrierenden synaptischen Gewichte werden durch die Position der Neuronen in beiden Schichten automatisch ausgerichtet. Resultate eines Experimentes zur Verknüpfung chinesischer Zeichen zu Alphabeten werden vorgestellt.

## 1. Introduction

The techniques of optical interconnections are extensively studied for the implementation of large-scale artificial neural networks. The artificial neural networks that have optical interconnections are called optical neural networks [1–9] and attract much attention by virtue of the speed and parallelism of light. The optical neural networks are categorized into holographic [4–7] and non-holographic types [1–4, 8, 9]. In the holographic type, synaptic weights are recorded on a hologram in the distributed mode of representation. In the non-holographic type, they are usually recorded on an SLM in the localized mode of representation. It is clear that these types of large-scale optical neural networks have the considerable difficulty of aligning their optics because of the possible high density of interconnections and the remaining aberrations of optics. An alignment-free technique is expected to remove this difficulty. In one of the holographic optical neural networks [5], an alignment-free technique was used. The interconnections are realized by holographic gratings in a photorefractive crystal. The holographic

gratings are formed with optical beams from artificial neurons in the front and rear layers. In the non-holographic type of optical neural networks, however, no alignment-free techniques have been proposed.

In this paper, we propose a lateral-alignment-free technique for an optical neural network. We optically implement Willshaw's type of network [10] without the use of holograms. In this network, input and output signals and synaptic weights are represented by binary values. We examined experimentally the alignment-free technique. The results are presented in section 3. In the experiment, the technique of sparse encoding [11] is used. An improved version of the first network of ADAM (advanced distributed associative memory [12]) is used for the sparse encoding of input patterns.

## 2. Alignment-free optical neural network

The principle of the present alignment-free optical neural network will be illustrated in this section. Signal processing process in this network is similar to that of the usual optical neural networks. The learning process is, however, different. This process makes the optical system free from the strict alignment in the plane normal to the optical axis.

### 2.1. Architecture and signal processing

We adopted Willshaw's network [10] to realize the alignment-free technique. In the processing mode of the Willshaw's network, the operations of binary vector-matrix multiplication and thresholding are necessary. Let  $x$  and  $y$  denote the input and output pattern vectors, and let  $W$  denote synaptic weight matrix. The operation of the network is then written as,

$$y = f(Wx), \quad (1)$$

where  $f(\bullet)$  denotes the componentwise operation of thresholding. In the present alignment-free optical neural network, we employ the spatial coding method [8] proposed by Ishikawa et al. to execute eq. (1). This method can treat two-dimensional input patterns without rearranging them into one dimensional pattern vector (see ref. [8]).

An ideal model of the alignment-free optical neural network is shown in fig. 1. Each artificial neuron in the input layer has a light transmitter, whereas each neuron in the output layer is assumed to have a light transmitter/receiver (photo-transceiver). In the processing mode, when the input pattern is fed to the input layer, the array

Received June 7, 1994.

Norimichi Tsumura, Yusaku Fujii, Kazuyoshi Itoh, Yoshiki Ichioka, Department of Applied Physics, Osaka University, Yamada-oka 2-1, Suita, 565 Japan

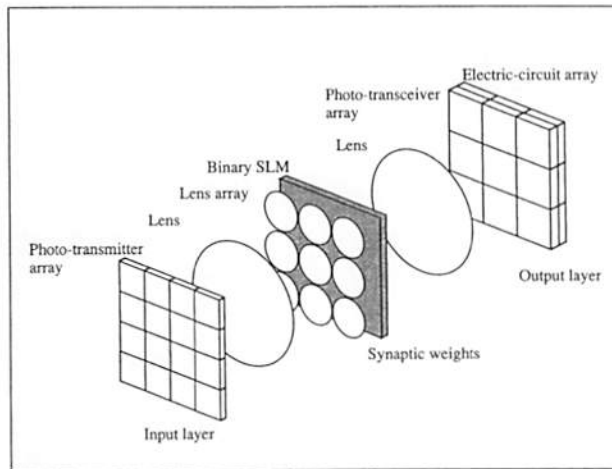


Fig. 1. Ideal model of alignment-free optical neural network with no holograms.

of photo-transmitters in the input layer transmits optical input signals to Binary SLM. The first single lens and an array of lenses are used to form multiple images of an input pattern for the spatial coding. The SLM that memorizes binary values of the optical transmittance is placed in the image plane of the multiple imaging system. We assume here a transmission type of SLM. After training, the synaptic weights are memorized in this SLM as a 2-D pattern of optical intensity modulations. Each modulation in this SLM is binary i.e., the incident light is allowed to pass (state 1) or not (state 0). We assume that the states of 0 and 1 correspond to the synaptic weights of 0 and 1, respectively. The multiple images of the input pattern are modulated by the synaptic weights. We will show later that the 2-D pattern, that is recorded on the SLM and acts as the synaptic weight matrix, is automatically located at the exact position for modulating the multiple images. The modulated multiple images are imaged onto an array of photo-transceivers. Each photo-transceiver detects the total power incident on its aperture. The VSTEP (vertical-to-surface transmission electro-phonic device) [13] is an example of this ideal photo-transceiver. The detected optical signals are compared with a threshold in an array of electronic circuits. This array of circuits produces a binary pattern as an output.

## 2.2. Automatic optical alignment in the learning mode

In the learning mode, training sets are fed successively to the network. The training sets are desired pairs of input and output patterns. The arrays of photo-transmitters in the input and output layers send optical signal to the SLM, simultaneously. Fig. 2 illustrates the important property of alignment-free recording of synaptic weights in the learning mode. Multiple images ( $3 \times 3$ ) of the input pattern ( $x$ ) that are composed of  $4 \times 4$  outputs ( $x_i$ ) of the neurons ( $i$ ) in the input layer are projected onto the SLM. The desired output pattern ( $r$ ) of the training pair that is composed of  $3 \times 3$  signal elements ( $r_j$ ) is projected from

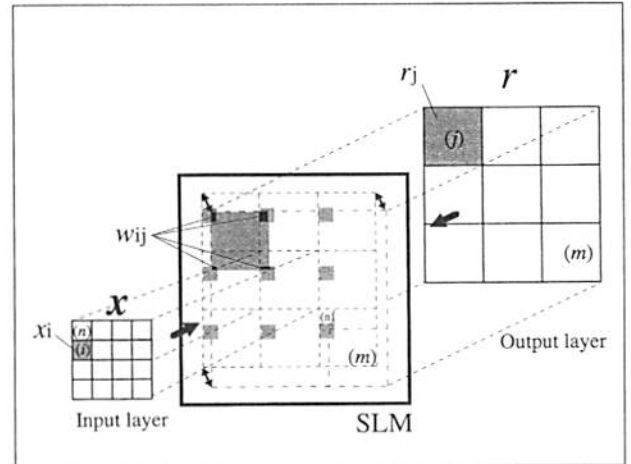


Fig. 2. Illustration of a recording process of synaptic weights in the present optical neural network.

the neurons ( $j$ ) in the output layer at the opposite side of the SLM. We assume that the SLM functions to produce and keep the two-dimensional product of AND-operations between the multiple images of the input pattern and the image of the output pattern. That is, the synaptic weights are recorded at positions where the signals of the both patterns of  $3 \times 3$   $x$ 's from the input layer and  $r$  from the output layers meet on the SLM. The synaptic weight ( $w_{ij}$ ) is recorded on the SLM at the locations determined by the signals of  $x_i$ ,  $r_j$ , as in fig. 2 (deep-black areas). Note that fig. 2 illustrates the case where the input and output patterns ( $x$  and  $r$ ) are not exactly aligned. If the optical system is precisely aligned, each multiple image is completely fitted into one of the element of the projected image from the desired output pattern. In the present case, the synaptic weight ( $w_{ij}$ ) is split into four parts. Nevertheless, signals are correctly processed in the processing mode. Suppose that an input signal ( $x_i$ ) is fed to the input layer in the processing mode. The input pattern is assumed to be placed at exactly the same position in the optical system. This assumption is an important requirement for the consistency of the alignment-free recording of synaptic weights. If this requirement is met, the input signal passes through exactly the same position where the synaptic weight ( $w_{ij}$ ) is recorded in the learning mode. The signal reaches to the output neuron ( $j$ ) on the basis of an "optical reciprocity" [14]. This property is preserved in any case, if the optical system is not deformed after the learning process.

The present system has, however, a problem; signals from some neurons in the input layer are not interconnected optically to neurons in the output layer. A condition, that the projected area from an output neuron include at least one signal that is projected from an input neuron, must be satisfied to interconnect the input and output neurons optically. For example, suppose that neuron ( $n$ ) is located at the upper left corner in the input layer, and neuron ( $m$ ) is at the lower right corner in the output layer as in fig. 2. The neurons ( $n$ ) and ( $m$ ) are not

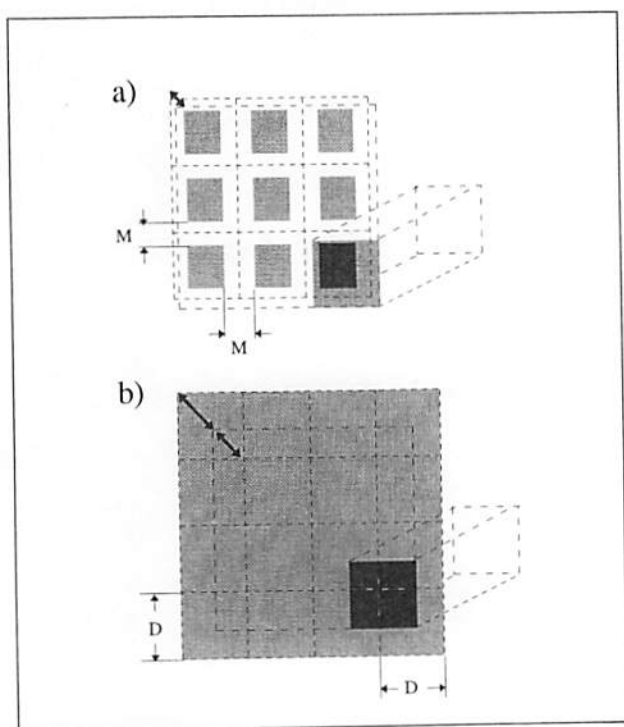


Fig. 3. Methods to satisfy the optical connectable condition in all pairs of neurons in the input layer and in the output layers.

interconnected optically, because the above condition of optical interconnection is not satisfied. Fig. 3 shows two types of methods by which the condition of optical interconnection is satisfied. The multiple images that are projected on the SLM from the input layer and the image of the output layers with a specific neuron are drawn in fig. 3. In one method, a margin is given between the input images that are set side by side as in fig. 3a). Suppose the length of the margin is  $M$ , then the alignment of optical system has the same amount of tolerance. In the other method, the projected area from the input layer is extended by additional multiple images that are produced by additional lenses in the lens array. Suppose the width of the additional area is  $D$  on the SLM, the lateral-alignment of the optical alignment is  $D$ . In the experiment shown in the next section, the former method is used.

We also assume that repetition of this AND-operation results in overwriting of the successive products on the SLM. In other words, OR-operations are carried out between the recorded and current signals. This assumption promises training of many associations. Suppose that  $n$ -th training pairs is presented to the network. Let  $x_i^n$  and  $r_j^n$  denote, respectively, signals at pre-synaptic neuron ( $i$ ) in the input layer and at the post-synaptic neuron ( $j$ ) in the output layer. The new synaptic weight ( $w_{ij}^n$ ) associated with neurons ( $i$ ) and ( $j$ ) in the input and output layers of the present neural network can be written as,

$$w_{ij}^n = w_{ij}^{n-1} \cup (x_i^n \cap r_j^n), \quad (2)$$

where all the variables are binary,  $\cap$  and  $\cup$  denote the AND- and OR-operations, respectively. The initial synap-

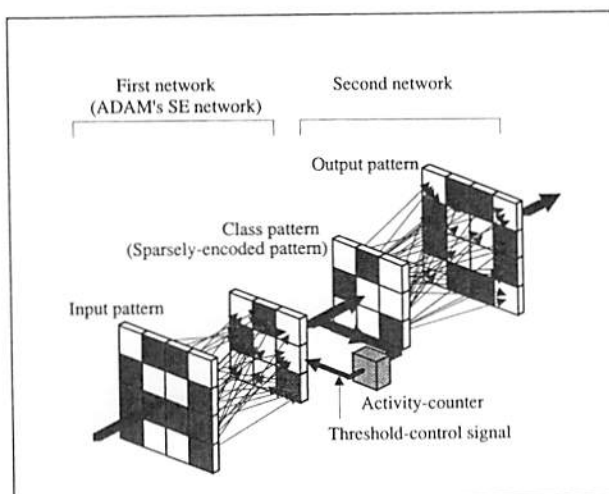


Fig. 4. Architecture of ADAM.

tic weight ( $w_{ij}^0$ ) for all  $i$  and  $j$  is set to be zero. This training method of synaptic weights produces the same value of synaptic weights which are decided by the Willshaw's method [10].

A ferroelectric-liquid-crystal (FLC)-SLM [15, 16] that is optically addressable can execute above operations and can be used as the SLM in the present system. When an electric control pulse is applied, the transmittance of the SLM is altered from low to high due to the rotation of FLC molecules at the positions where intensities of incident light exceed a certain threshold. This recording threshold can be changed by controlling height and/or width of voltage of the electric pulse. The recording threshold can be adjusted so that AND-operation is exactly executed between the multiple images from the input layer and the image from the output layer. The spatial distribution of rotation angle of molecules is kept constant or memorized if no electric control pulse is applied. The OR-operation can readily be executed because the SLM memorizes the spatial distribution of intensity modulation additively.

### 3. Experiments

We made a preliminary experiment to examine the present alignment-free technique. In addition, we improved the Willshaw's network by incorporating a sparsely-encoding section at the front end of the network to improve the capacity of associations.

#### 3.1. Improvement of Willshaw's network by sparsely-encoding network for the experiment

In the Willshaw's network, neurons in the output layer have a constant threshold. This threshold is adjusted according to the activity in the input layer. The activity is defined as the number of active neurons in the receptive field, or the number of elements that have value 1 in the vector of input pattern. If the activities of the input pat-

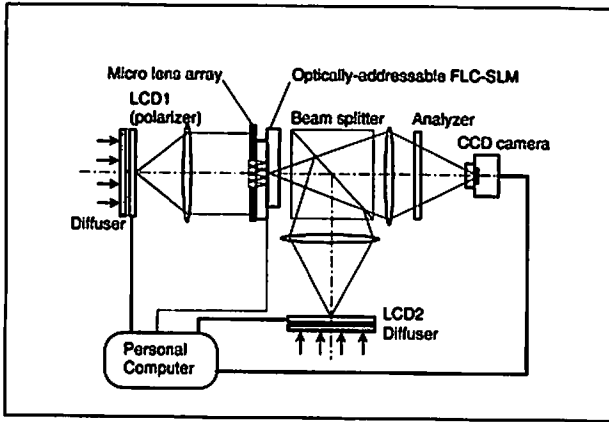


Fig. 5. Configuration of the experimental system.

terns are allowed to change from pattern to pattern, it is difficult to fix an appropriate threshold in the output layer. This difficulty was removed in ADAM [12]. The architecture of the ADAM is shown in fig. 4. In the output layer of the first network of ADAM, the threshold of each neuron is always controlled by a signal from the activity-counter, so that the activity of the output layer is kept constant. The first network encodes input patterns to class patterns [12] that have constant activity, and the second network associates output patterns with the class patterns. The technique of sparse encoding [11] improves the storage capacity of the ADAM [12]. The activities of class-patterns are small in the case of sparse encoding. Such the network may be called sparsely-encoding (SE) network. The output layer of the SE network is called here a sparsely-encoding layer, and the class patterns are called sparsely-encoded patterns.

In the experiments, we use an improved ADAM's SE network. The synaptic weights of the SE network are trained by input patterns in the training sets. The initial synaptic weights are binary and randomized. Suppose we present  $n$ -th training set to the network. When  $x_i^n$  and  $f_j^n$ , respectively, denote the signals at neuron ( $i$ ) in the input layer and neuron ( $j$ ) in the sparsely-encoding layer, the synaptic weight ( $m_{ij}^n$ ) between these neurons is modified as,

$$m_{ij}^n = m_{ij}^{n-1} \cap (x_i^n \cup \bar{f}_j^n), \quad (3)$$

where all variables are binary,  $\bar{f}$  denotes the logical complement of  $f$ . Note that the synaptic weights are pruned during this training procedure. When we use this network in the processing mode, we can eliminate the neurons that show no activity in this training procedure.

We can show that the improved SE network can be implemented by present alignment-free technique. In the implementation, the erasing mode of FLC-SLM may be used. In the erasing mode, the optical modulation switches to state 0 regardless of the previous state when an optical signal above a threshold arrives. If we take the complement of eq. (3) and use de Morgan formulas, we can see that a reversal of an input pattern may be used along with the FLC-SLM in the erasing mode. The activity-counter can be implemented electrically in the part of electronic circuit array [17].

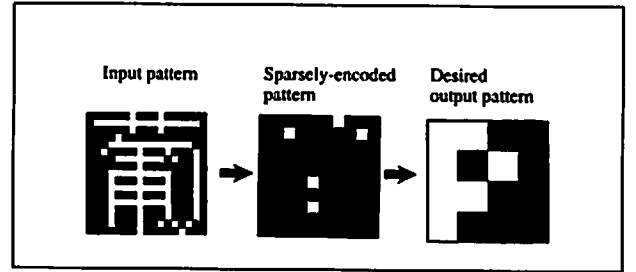


Fig. 6. An example of training sets (desired pairs of input patterns and output patterns) and sparsely-encoded patterns of the desired input patterns.

### 3.2. Optical system

The configuration of the experimental optical system is shown in fig. 5. In this experiment, the SE network is simulated by a personal computer because optical implementation requires the lens array of  $17 \times 17$  elements. An array of  $4 \times 4$  elements was only available at the time of experiment. A liquid-crystal-display (LCD1) illuminated by an incoherent light source functions as an array of photo-transmitters for the neurons in the input layer. An LCD2 and the charge-coupled-device (CCD) camera are coupled together by a beam splitter (BS) so that they act together as an array of the photo-transceivers. In this system, the condition of optical interconnection is satisfied by the method described in sec. 2.2 by referring to fig. 3a). The lateral tolerance of 1.8 mm was given in this system, i.e. the margins between the projected input images are approximately 1.8 mm. Let us consider the process of training the optical section of the present network. Suppose that the sparsely-encoding network implemented in the personal computer is already adapted to the training patterns. Then, the sparsely-encoded patterns are displayed on the LCD1, while the desired output patterns are displayed on the LCD2. We used LAPS-SLM [16] as an optically addressable FLC-SLM. We used an array of  $4 \times 4$  graded-index micro lenses (SELFOC micro lenses [18]) for the multiple imaging of the input pattern. The focal length of the micro lens is so determined that the lens array makes an array of images in the sensitive layer of the LAPS-SLM when the array is brought into direct contact with the LAPS-SLM. The diameter of a SELFOC micro lens is 2.0 mm. The thickness and the focal lengths are 2.61 mm and 5.89 mm, respectively. From the image taken by the CCD camera, the personal computer simply sums up the modulated optical signals for each neuron in the output layer and binarizes the sum. The personal computer also sends the control electric pulse to the LAPS-SLM.

### 3.3. Experimental results

We carried out an experiment of associations from Chinese characters to alphabets. The size of the Chinese characters is  $17 \times 17$  pixels, and that of the alphabets is  $4 \times 4$  pixels. In the sparsely-encoding layer,  $15 \times 15$  neurons are used. The alphabetical characters that are de-

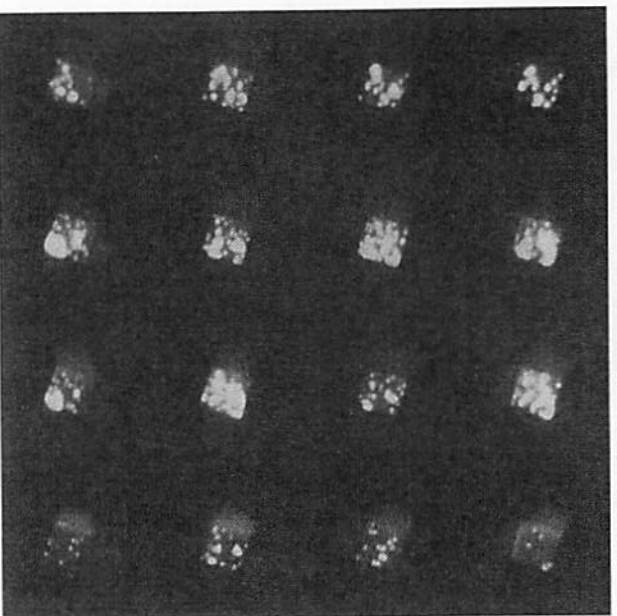


Fig. 7. Synaptic weights on LAPS-SLM after training. (The area of view is approximately  $1 \times 1 \text{ cm}^2$ ).

sired output patterns are so designed that all the alphabets have the same activity. This designing improves the storage capacity of the network [19]. An example of the training sets and their sparsely-encoded patterns used in the experiment are shown in fig. 6. The 3600 optical interconnections that are necessary for all the association experiment have been successfully achieved. In the experiment, the 14 training sets are completely memorized.

Synaptic weights that are recorded on LAPS-SLM after training are shown in fig. 7. Note that the sparsely-encoded patterns are rotated on the LAPS-SLM. The LCD1 is inclined approximately 20 degree so that the azimuth of polarization of input optical signal coincides with that of liquid crystal molecules in the LAPS-SLM. Fig. 7 covers an area of approximately  $1 \times 1 \text{ cm}^2$  of LAPS-SLM. It is shown that the high density of successive optical recording is achieved without strict alignment. The density of recording is at most 300 pixels/ $\text{mm}^2$  on the SLM. It should be noted that such an exact alignment might be impossible in practice without the help of the alignment-free technique. The storage capacity of our experimental system is practically limited by the blurring of the recorded synaptic weights on the LAPS-SLM. The blurring occurs after several repetitions of recording sparsely-encoded patterns. In fig. 7, we can see that the blurring occurs at the positions where many sparsely-encoded patterns are overwritten.

We then examined the robustness of the trained network against random noise. Input patterns with random noise are presented to the optical neural network with the SE network which has been trained by the training sets without noise. Fig. 8 presents experimental results about robustness of the network; the fraction of correct associations is plotted as a function of fraction of noise. We can see that the present system is robust against small frac-

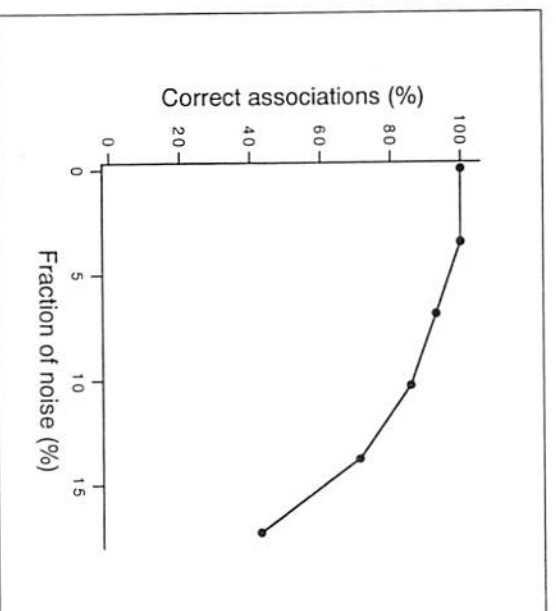


Fig. 8. Experimental results about robustness of the network.

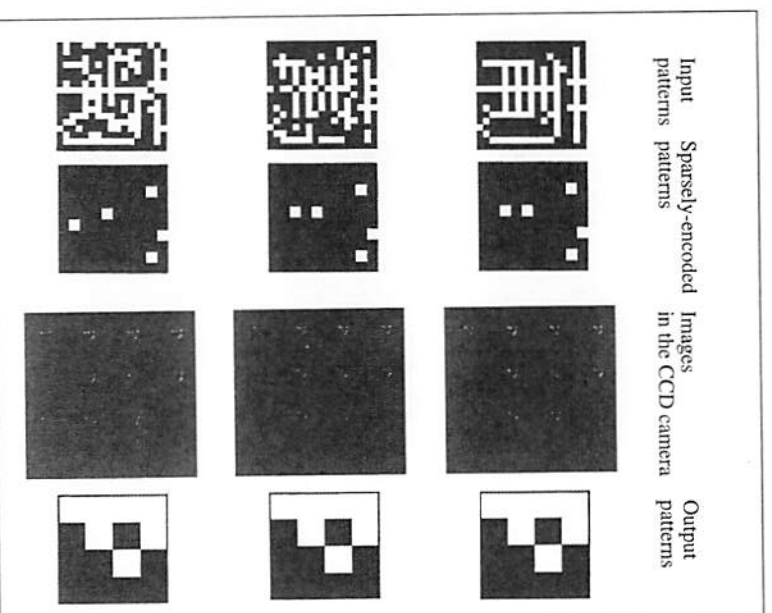


Fig. 9. Examples of associations of patterns with noise. (The top row is for 0% noise, the middle and bottom row are for 10% and 17% noise, respectively).

tion of noise. The examples of associations under the presence of noise are shown in fig. 9. The top row shows the process of association for the input pattern of 0% noise, the middle and bottom rows are for the patterns of 10% and 17% noise, respectively. It is shown that sparsely-encoding process is sufficiently robust against the noise of 10%, and no bit is changed in the sparsely-

encoded pattern. In the case of 17% noise, however, the sparsely-encoded pattern is changed slightly. Nevertheless, the final association is perfect. We see that the robustness of associations against noise is enhanced by the two-stage architecture. It is noted finally that without the SE network only 3 patterns in 14 training patterns were correctly memorized in the network system.

#### 4. Discussions and conclusion

We have proposed an alignment-free technique of a non-holographic type of optical neural networks. The most important factor of this technique is that products of AND-operations in the training procedure are obtained and overwritten in the SLM, simultaneously. By the use of present self-aligning technique, we can overcome the difficulty of alignment that is essential for large-scale optical neural networks. The high density of the optical recording that is at most 300 pixels/mm<sup>2</sup> on the SLM is achieved in the present experiment.

In the presented optical neural network, we need to adjust carefully the focus of multiple images in the optical system, although we do not need to align most of the components in the optical system. Defocusing of multiple images results in the waste of high spatial resolution inherent in the SLM. An optical packaging technique [20, 21] may eliminate the need for the focusing.

#### Acknowledgment

The authors would like to thank Tadao Iwaki and Syuhei Yamamoto in Seiko Instruments Inc. for providing the LAPS-SLM. The authors also would like to thank Kenji Hamanaka in Nippon Sheet Glass Company, Ltd. for providing the SELFOC micro lens array.

#### References

- [1] D. Psaltis, N. Farhat: Optical information processing based on an associative-memory model of neural nets with thresholding and feedback. *Opt. Lett.* 10 (1985) 98–100.
- [2] N. H. Farhat, D. Psaltis, A. Prata, E. Paek: Optical implementation of Hopfield model. *Appl. Opt.* 24 (1985) 1469–1475.
- [3] A. D. Fisher, R. C. Fukuda, J. N. Lee: Implementation of Adaptive Associative Optical Computing Elements. *Proc. SPIE* 625 (1986) 196–204.
- [4] A. D. Fisher, W. L. Lippincott, J. N. Lee: Optical implementations of associative networks with versatile adaptive learning capabilities. *Appl. Opt.* 26 (1987) 5039–5054.
- [5] K. Wagner, D. Psaltis: Multilayer optical learning networks. *Appl. Opt.* 26 (1987) 5061–5076.
- [6] D. Psaltis, D. Brady, K. Wagner: Adaptive optical networks using photorefractive crystals. *Appl. Opt.* 27 (1988) 1752–1759.
- [7] C.-H. Wang, B. K. Jenkins: Subtracting incoherent optical neuron model: analysis, experiment, and applications. *Appl. Opt.* 29 (1990) 2171–2186.
- [8] M. Ishikawa, N. Mukohzaka, H. Toyoda, Y. Suzuki: Optical association: a simple model for associative memory. *Appl. Opt.* 28 (1989) 291–301.
- [9] T. Lu, S. Wu, X. Xu, F. T. S. Yu: Two-dimensional programmable optical neural network. *Appl. Opt.* 28 (1989) 4908–4913.
- [10] D. J. Willshaw, D. P. Buneman, H. C. Longuet-Higgins: Non-Holographic Associative Memory. *Nature* 222 (1969) 960–962.
- [11] S.-I. Amari: Characteristic of Sparsely Encoded Associative Memory. *Neural Networks* 2 (1989) 451–457.
- [12] J. Austin, T. J. Stonham: Distributed associative memory for use in scene analysis. *Image and Vision Computing* 5 (1987) 251–260.
- [13] K. Kubota, Y. Tashiro, K. Kasahara, S. Kawai: Optical Crossbar Interconnection Using Vertical-to-Surface Transmission Electro-Photonic Devices (VSTEP). *Proc. SPIE (Optical Computing 88)* 963 (1988) 255–259.
- [14] M. Born, E. Wolff: *Principles of Optics – sixth edition*. Pergamon Press, Tokyo, 1980.
- [15] K. M. Johnson, G. Model: Motivations for using ferroelectric liquid crystal spatial light modulators in neurocomputing. *Appl. Opt.* 28 (1989) 4888–4899.
- [16] S. Yamamoto, R. Sekura, J. Yamanaka, T. Ebihara, N. Kato, H. Hoshi: Optical Pattern Recognition with LAPS-SLM (1)/Light Addressed Photoconductor and Smectic C\* Liquid Crystal Spatial Light Modulator. *Proc. SPIE (Computer and Optically Formed Holographic Optics)* 1211 (1990) 273–283.
- [17] T. M. Slagle, K. Wagner: Winner-take-all spatial light modulator. *Opt. Lett.* 17 (1992) 1164–1166.
- [18] K. Matsushita, M. Toyama: Unevenness of illuminance caused by gradient-index fiber arrays. *Appl. Opt.* 19 (1980) 1070–1075.
- [19] H. Toyoda, M. Ishikawa: Sparse Encoding Algorithm for Optical Associative Memory Using Bistable Spatial Light Modulator. *Proceeding of the 12th International Display Research Conference*, October 12–14 (1992) 371–374.
- [20] K. Hamanaka: Optical bus interconnection system using Selfoc lenses. *Opt. Lett.* 16 (1991) 1222–1224.
- [21] D. Miyazaki, J. Tanida, Y. Ichioka: Reflective block optics for optical computing systems. (Eds.): *Optical Computing*, 1993, *Technical Digest Series*. 30–33. Optical Society of America, Palm Springs, California 1993.